Chapter 4

Self-Organized Nanopore Arrays of AAO Films

4.1 Introduction

For the template applications, it is highly favorable to arrange the anodic aluminum oxide (AAO) pore channels into a two-dimensional (2-D) lattice with long-range order. However, the initially formed nanopores nucleate randomly, resulting in irregular pore arrangement on the surface and curved pore channels. Some successful strategies have recently been proposed to improve the periodicity of the AAO nanopores. Masuda *et al.*[Masuda 1997-2770; 2001-189] have reported the development of nanopores in pre-textured aluminum, where the shallow concaves formed by SiC mold indentation work as pinning points for guiding the growth of nanochannels. The obtained AAO has a perfectly ordered array of straight parallel channels perpendicular to the surface. Similarly, focus-ion-beam (FIB) lithography can also be used to create concaves on an aluminum surface and the concaves initiate the development of nanopores in the following anodization step[Liu 2001-120; Liu 2003-1281]. However, these lithographic-guiding techniques involve many drawbacks such as low yield, high equipment cost, and incompatible with integrated circuit (IC) technology. A conveniently means by the name of two-step anodization is another choice for producing the ordered pore channels[Masuda 1995-1466; 1996-L126]. Because the anodization of aluminum into AAO is accompanied by the volume expansion, the strain energy from the volume expansion causes that the nanopores organize spontaneously into a hexagonally close-packed (hcp) arrangement[Li 1998-6023]. Under specific anodization conditions, a highly ordered array of the nanopores can also be obtained on the premise that the anodization is performed for a long time. However, the nanopores are grouped into domains with domain sizes in the range of a few micrometers and the ordered arrangement of the nanopores is disrupted by the domain boundaries (short-range order). In this study, the two-step anodization was conducted to produce the AAO template with ordered nanopores. Moreover, the AAO template was prepared directly on aluminum films coated on silicon wafers aiming at integrated microelectronic applications, which has met with little success because of

poor aluminum film quality and/or limited aluminum film thickness. The majority of previous studies used aluminum foils to prepare the nanoporous films, which must eventually be separated from the aluminum foil for later applications[Mei 2002-361; Wang 2004-816]. This is apparently not suitable for most integrated device applications.

4.2 Al film electropolishing

For the fabrication of the nanoporous AAO film, a high purity aluminum film (99.999%) with a thickness of about 6 μm was first deposited on a (100)-oriented *p*-silicon wafer by thermal evaporation in a high vacuum chamber with a base pressure of 5×10^{-7} Torr. Figure 4-1 shows the atomic force microscopy (AFM) (Digital Instruments NanoScope Ⅱ) images of the as-deposited aluminum surface. The

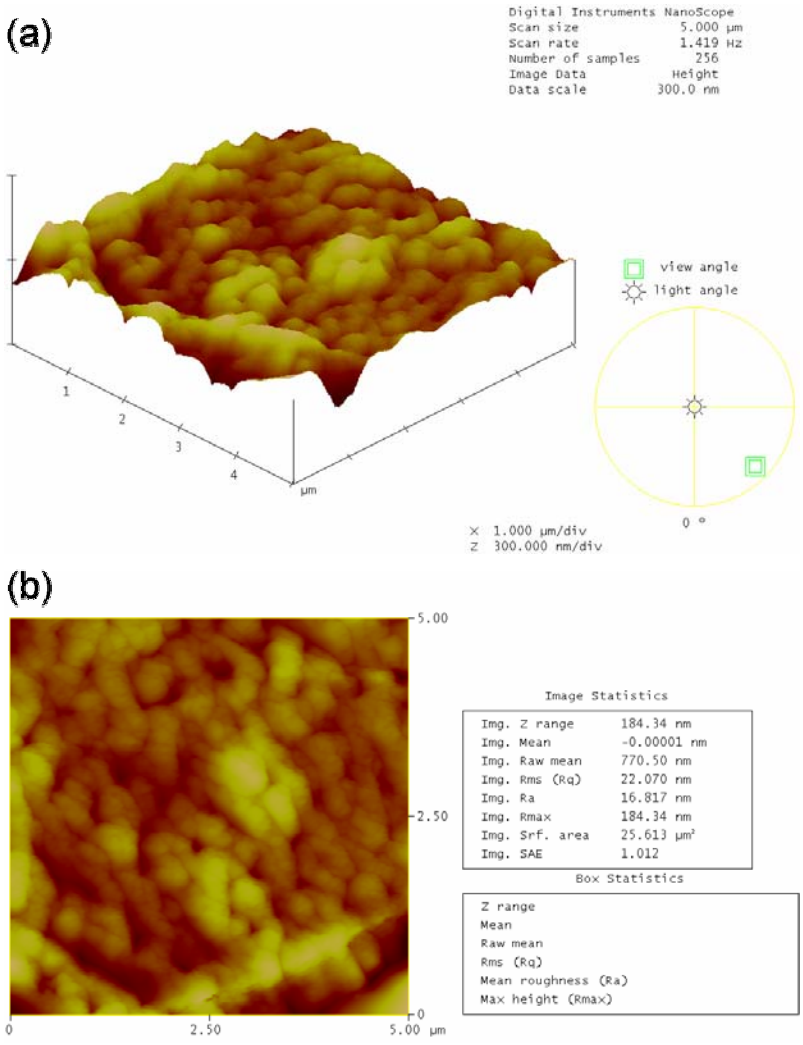

Figure 4-1 Contact-mode AFM images (5×5 μm^2) of the as-deposited aluminum film surface: (a) 3D diagram; (b) roughness analysis.

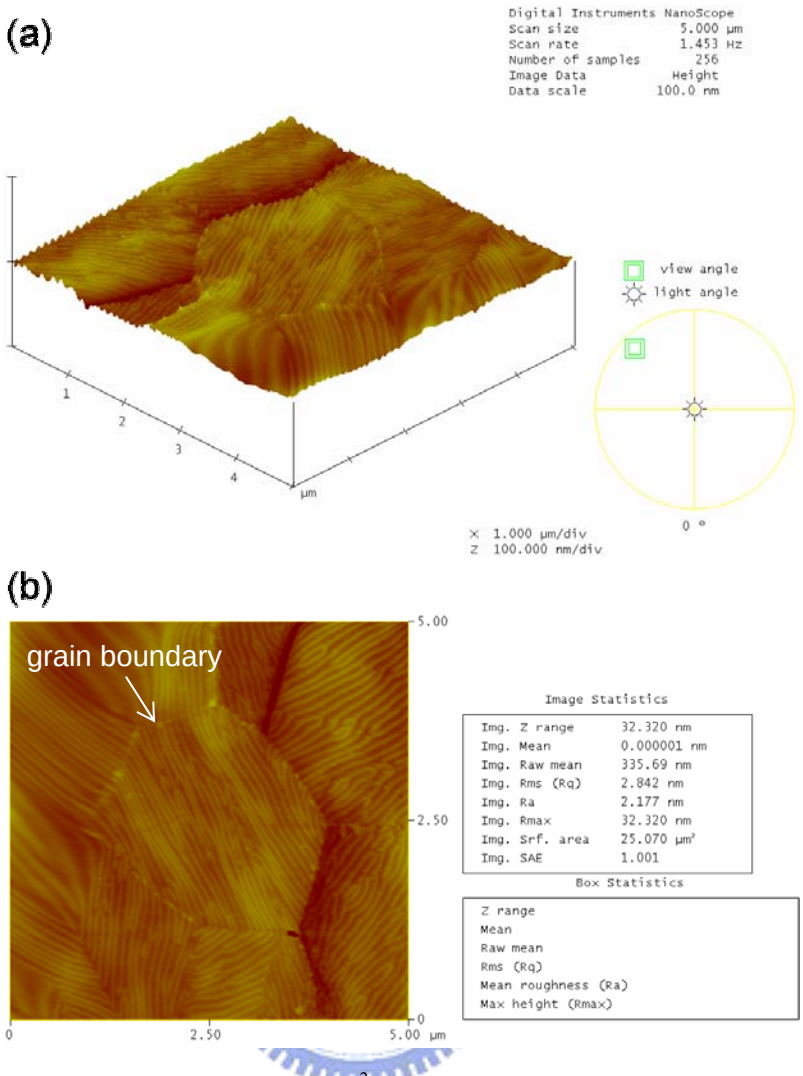

Figure 4-2 Contact-mode AFM images (5×5 µm^2) of the aluminum film surface after the electropolishing for 7 sec: (a) 3D diagram; (b) roughness analysis.

aluminum film exhibits surface roughness in µm scale, which must be polished to obtain a smooth, scratch-, and stress-free surface prior to anodization. Because mechanical polishing is not suitable for thin film planarization, in this study, electropolishing was introduced to reduce the surface roughness of the aluminum film. Electropolishing is a surface finishing process based on anodic dissolution of a metal in an adequate electrolyte. The mechanism of electropolishing has not yet been fully determined, but it is usually explained as the microleveling effect owing to selective dissolution[Chang 2003-58]. When the anodic voltage is applied, the passivation layer covers the concave areas of the surface leading to a lower dissolution rate. However, the protrusion areas of the surface does not be covered with the passivation layer resulting in that the areas receive greater current from the cathode and thus have a higher dissolution rate. The surface roughness of the polished film will gradually be reduced under the specific

electropolishing conditions with the passivation layer formation. However, evidence concerning this inert layer needs more investigation.

Figure 3-2 shows the schematic diagram of experimental setup for the aluminum electropolishing. The electrolyte was a mixed solution of 25 vol.% perchloric acid ($HClO_4$) and 75 vol.% ethanol (C_2H_5OH). The perchloric acid is a strong oxidizer which was used to achieve the appropriate low *p*H to assure that aluminum ionizes into Al^{3+} and does not form other ions or oxides during the polishing reaction. As for the ethanol, it works as a high-kinematic-viscosity and wetting solvent for the ions involved in the dissolution[Yuzhakov 1997-608]. The electrolyte was violently stirred and maintained at a constant temperature of 21 ^{o}C by a cooling system. A constant polarization voltage of 40 V was applied to force the electrochemical reactions. Figure 4-2 shows the AFM images of the aluminum film surface after the electropolishing for 7 sec. After the electropolishing the large surface irregularities are significantly removed. However, the surface morphology of the polished aluminum film exhibits labyrinthine stripes interrupted by aluminum grain boundaries. Yuzhakov *et al.*[Yuzhakov 1997-608; 1999-62] have study the nanoscale pattern formation on aluminum surface during electropolishing. They proposed that the regular patterns are attributed to preferential adsorption of organic molecules on the bumps of the aluminum surface due to its enhanced electric field. This reduces the relative dissolution rate at the bumps and generates the patterns.

4.3 Two-step anodization

After the aluminum electropolishing, the two-step anodization, which is shown schematically in Figure 4-3, was used to prepare ordered pore channel arrays of AAO. The corresponding field-emission scanning electron microscopy (FE-SEM) (Hitachi S-4000) images of the two-step anodization process are shown in Figure 4-4. The experimental setup for the aluminum anodization is similar to that for the electropolishing shown in Figure 3-2. The porous AAO preparation is always performed in an acidic electrolyte in order to maintain the low *p*H condition and the electrochemical reaction kinetics. First anodization was carried out in a 0.3 M oxalic acid ($H_2C_2O_4$) solution at 21 ^{o}C under a constant polarization voltage of 40 V for 50 min. After the first anodization, the arrangement of the nanopores is not very regular and the diameter distribution of the nanopores is somewhat broad, as shown in Figure 4-4(a), although a rough pore arrangement along with the stripes formed during the

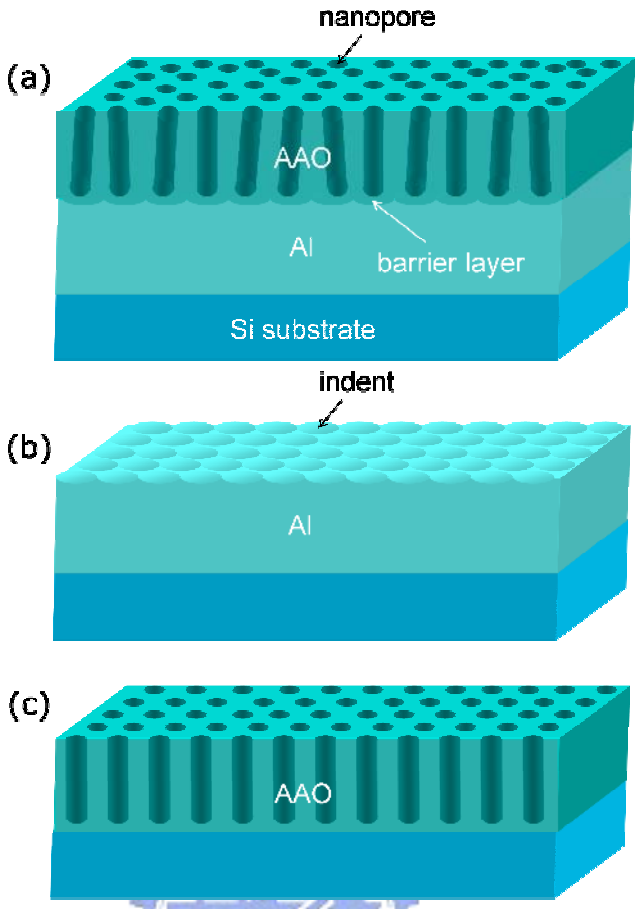

Figure 4-3 Schematic diagram of the two-step anodization process: (a) First anodization, (b) pre-textured aluminum film, and (c) second anodization.

electropolishing can be observed. After removing the AAO film formed in the first anodization step by wet chemical etching at 60 ^{o}C in a mixed solution of 6 vol.% phosphoric acid (H_3PO_4) and 1.5 wt.% chromic acid (CrO_3), a relatively ordered hexagonal pattern of hemispherical nanoindents was produced on the surface of the aluminum film [Figure 4-4(b)]. The hemispherical shape of the indents corresponds with the scalloped oxide barrier under each AAO pore bottom [Figure 4-5(a)]. The relative order in this scalloped surface suggests that longer anodization times lead to greater pore regularity in which self-organization of the randomly initiated pores can gradually take place. The hemispherical nanoindents on the aluminum surface will initiate the development of nanopores in the second anodization step, which will consequently yield the highly uniform nanopore arrays. The second anodization was performed under the same anodization condition as the first one. Figure 4-4(c) shows the top-view FE-SEM image of the AAO film after the two-step anodization and pore widening in a 5 vol.% phosphoric acid solution for 30 min. The resultant AAO film consists of highly ordered nanopores with a hexagonal arrangement. However, the

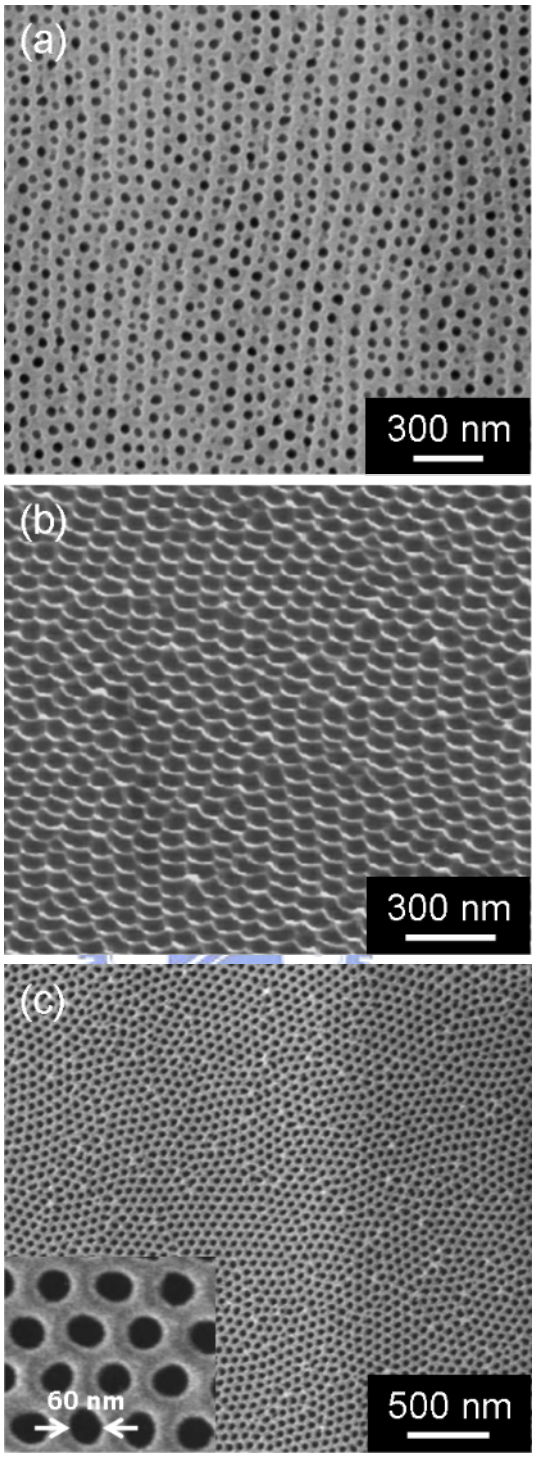

Figure 4-4 Top- or side-view FE-SEM images showing the two-step anodization process: (a) First anodization, (b) pre-textured aluminum film, and (c) second anodization and pore widening for 30 min. Anodization was conducted in 0.3 M oxalic acid at 40 V.

nanopores are grouped into domains and the periodical distributions of the nanopores are disrupted by the domain boundaries. The ordered domain sizes are determined by the time of the first anodization rather than the grain size of the initial aluminum film. As the initial aluminum film is thick enough, it permits a fairly long first anodization

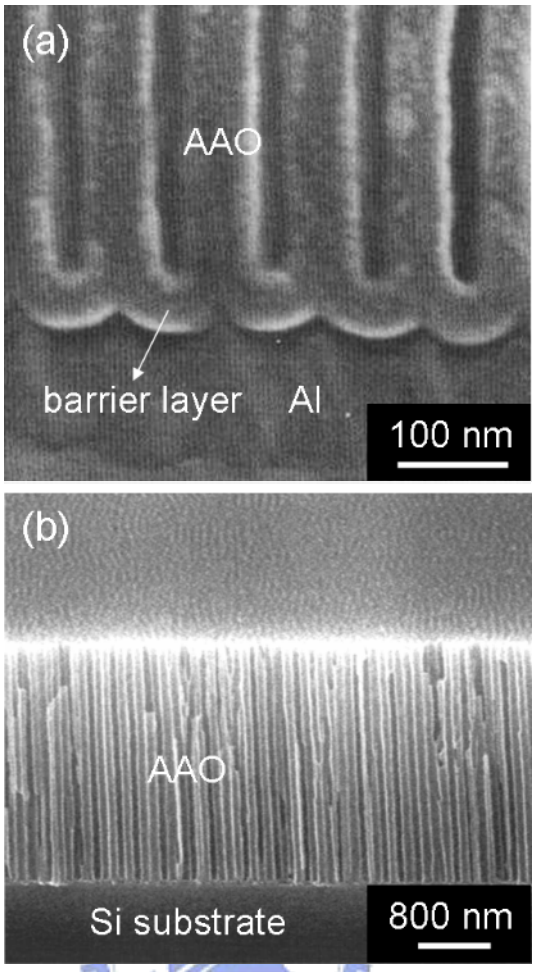

Figure 4-5 Cross-sectional view FE-SEM images showing (a) the aluminum oxide barrier layer and (b) the vertically aligned pore channels of AAO.

process for nanopore self-organization, and thus can result in a fairly large nanopore domain. The average domain size is a linear function of the time, which is very similar to metal grain growth. For grain growth at a constant temperature, the average grain radius (R_g) is a function of the time (t) described as

$$R_g = \Gamma t^n \tag{4.1}$$

where Γ is a temperature-dependent parameter and n is about 0.4-0.5[Li 1998-2470]. This empirical equation is also suitable for the nanopore domain growth during the anodization. The driving force for metal grain growth is the reduction of the grain boundary energy. With regard to the nanopore domain growth, the driving force is the mechanical stress associated with the volume expansion during the aluminum oxidation. The repulsive forces between neighboring pores at the metal/oxide interface drive the self-organized arrangement of the pores into closed-packed arrays[Jessensky 1998-1173].

The curves of anodic current density as a function of anodizing time for the

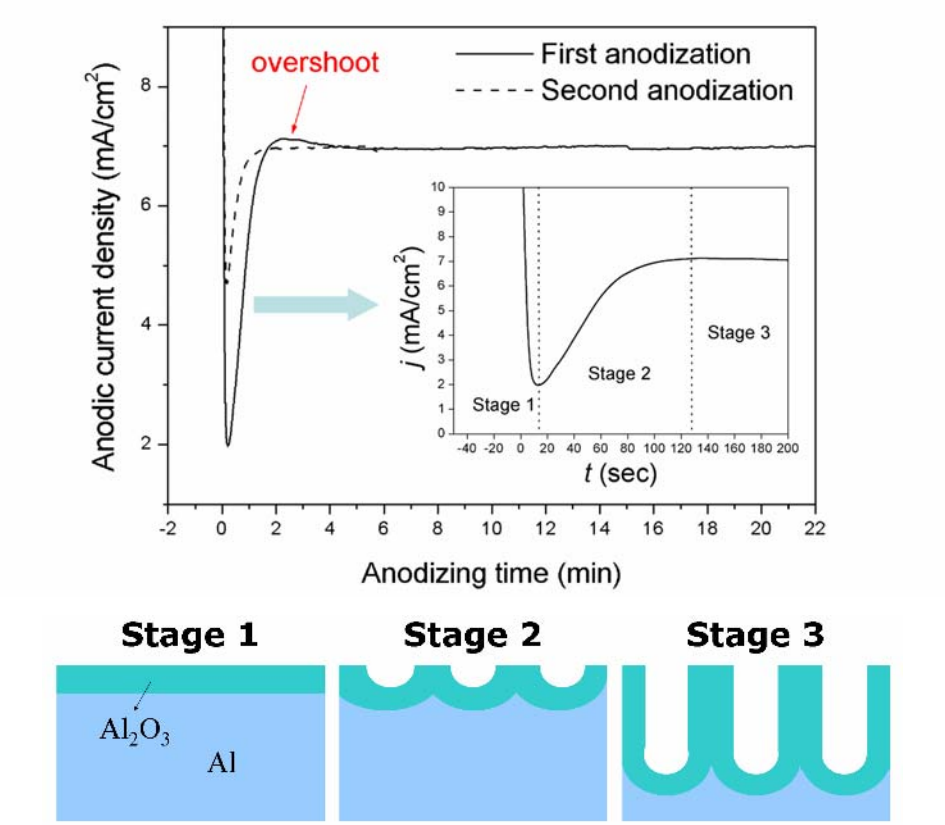

Figure 4-6 Anodic current density-anodizing time behaviors during the anodization of an aluminum film in a 0.3 M oxalic acid electrolyte. The insets are enlarged curve and schematic diagrams showing the anodization stages.

two-step anodization are shown in Figure 4-6, which can be divided into several stages. When the anodic voltage is applied, there is a barrier layer of aluminum oxide (Al_2O_3) grown on the aluminum surface (Stage 1). Then, tiny pores nucleate randomly through the oxide barrier with downward enlarged heads (Stage 2). Further anodization results in a steady-state growth of vertical pore channels containing scalloped hemispherical oxide barrier under each pore bottom (Stage 3), as shown in Figures 4-5. In the

Table 4-1 Detailed conditions for the aluminum anodizations.

Sample	A	B	C
Voltage	40 V	20 V	8 V
Electrolyte	$H_2C_2O_4$	H_2SO_4	H_2SO_4
Concentration	0.3 M	0.6 M	1.2 M
Bath temperature	21 °C	21 °C	21 °C
First anodization time	50 min	20 min	5 min
Pore widening time	60 min	10 min	10 min

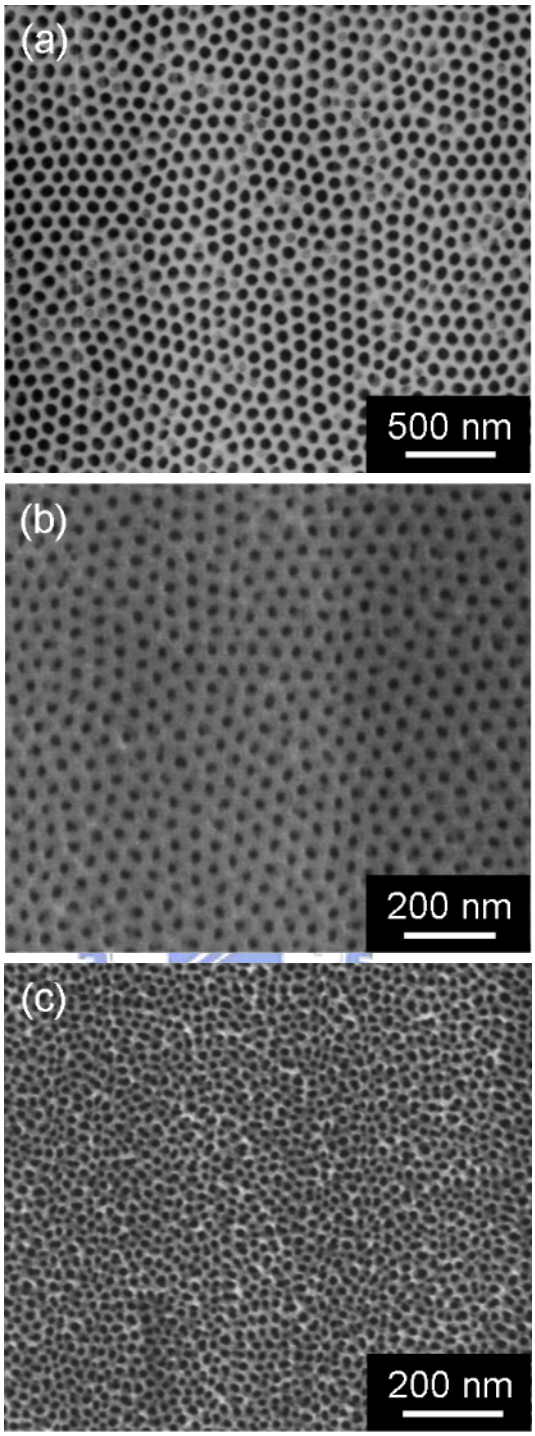

Figure 4-7 Top-view FE-SEM images of the nanoporous AAO films after the two-step anodization and pore widening. Anodization was conducted in (a) 0.3 M oxalic acid at 40 V (Sample A), (b) 0.6 M sulfuric acid at 20 V (Sample B), and 1.2 M sulfuric acid at 8 V (Sample C).

boundary between Stage 2 and Stage 3 of the first anodization, an overshoot phenomenon of the current density is always observed. When the initial pore nucleation is complete, a saturated pore density as high as 10^{12} cm^{-2} is obtained[Li 1998-2470], accompanied by a maximum current density, and then a slight decrease of current

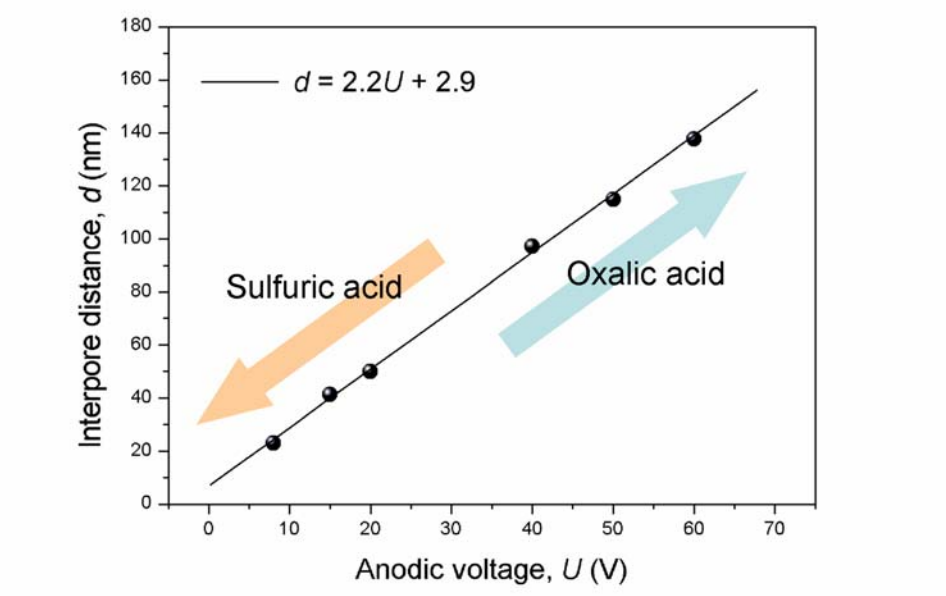

Figure 4-8 Average interpore distance as a function of anodic voltage for the nanoporous AAO films.

density is a consequence of the pores increase in size by merging with adjacent pores. However, for the second anodization (pre-textured aluminum surface), there is no current overshoot. Moreover, the minimum current density for the second anodization is larger than for the first anodization (as-polished aluminum surface). These obvious differences in the anodization behaviors are attributed to their diverse surface morphologies. Because there are nanosized indents with small radii of curvature on the pre-textured aluminum surface, the applied electric field is always concentrated on the indents. As a result the pore nucleation is easier inside the indent and is uniform, which is unlike the first anodization with random pore nucleation. Consequently, for the second anodization, less pore mergence occurs and thus no current overshoot was observed. On the other hand, the oxide thickness at the indent bottom is probably more thin and uniform than at the un-textured surface. Therefore, the second anodization has a higher minimum current than the first anodization.

The AAO pore size is a function of the anodic voltage and can be continuously varied in the range from ten to several hundred nanometers[Li 1998-6023]. In this study, the nanoporous AAO films with different interpore distances have been successfully prepared by regulating the anodic voltage and other conditions. The detailed conditions for the anodizations are summarized in Table 4-1. The pore structures of the nanoporous AAO anodized under the above conditions are presented in Figure 4-7. The average interpore distance increases linearly with anodic voltage as shown in Figure 4-8. The periodic pore arrangements with interpore distances of approximately 100, 50, and 23

nm were obtained in 0.3 M oxalic acid (Sample A), 0.6 M sulfuric acid (Sample B), and 1.2 M sulfuric acid (Sample C) solutions under voltages of 40, 20, 8 V, respectively. Almost perfect hexagonal ordered domains of the nanopores can be seen except for the Sample C. The dependence of the pore periodicity on the anodization conditions, e.g., anodic voltage, bath temperature, electrolyte species, and electrolyte concentration, has been studied. It was reported that the volume expansion of the aluminum during oxidation has a major effect on the periodic arrangements, which is varied with the anodization conditions, and the best ordered arrangements are observed when the volume expansion factor is about 1.4, independent of which electrolyte is used[Li 1998-6023; Jessensky 1998-1173]. According to this reason, the Sample C without growing ordered nanopores may ascribe to its volume shrinkage or immoderate volume expansion. Moreover, the Sample C was anodized in a concentrated sulfuric acid of 1.2 M with a very high reaction rate, causing that the first anodization was only performed for 5 min. Because the ordered domain size of nanopores depends strongly on the anodizing time, a short processing of the first anodization can also lead to the disordered nanopore arrangement.

4.4 Summary

Highly ordered nanopore arrays of AAO films have been successfully fabricated on silicon substrates by direct anodization of a thick aluminum film deposited on a silicon substrate. After the aluminum electropolishing, the two-step anodization of the aluminum film was introduced to produce the nanoporous AAO film with hexagonally arranged nanopores. The pore arrangements show polycrystalline structures with ordered domains in the diameters of a few micrometers (short-range order). The formation of the ordered hexagonal pore arrays is responsible for the volume expansion of aluminum during oxide formation causing repulsive forces between the neighboring pores which promote the self-organization of the pores. By tuning the anodic voltage and other anodization conditions, the pore arrays of AAO films with 20-150 nm interpore distances can be obtained.